tvst

Retina

Identifying Imaging Predictors of Intermediate Age-Related Macular Degeneration Progression

Rita Flores[1,2], Ana C. Fradinho[2], Rita Serras Pereira[1], Jorge M. Mendes[3], Miguel C. Seabra[2,4], Sandra Tenreiro[2], and Ângela Carneiro[5,6]

[1] Centro Hospitalar de Lisboa Central EPE, Department of Ophthalmology, Lisboa, Portugal
[2] iNOVA4Health, NOVA Medical School|Faculdade de Ciências Médicas, NMS|FCM, Universidade Nova de Lisboa, Lisboa, Portugal
[3] NOVA Information Management School (NOVA IMS), Universidade Nova de Lisboa; Campus de Campolide, Lisboa, Portugal
[4] University College London Institute of Ophthalmology, London, UK
[5] Centro Hospitalar Universitário de São João, Department of Ophthalmology, Portugal
[6] Department of Surgery and Physiology, Cardiovascular R&D Center, Faculty of Medicine of University of Porto, Porto, Portugal

Correspondence: Rita Flores, Medical Retina Service, Department of Ophthalmology, CHULC – Centro Hospitalar Universitário de Lisboa Central, Alameda de Santo António dos Capuchos, 1169-050 Lisboa, Portugal. e-mail: ritamariaflores@gmail.com

Received: March 5, 2023
Accepted: June 23, 2023
Published: July 25, 2023

Keywords: intermediate AMD; progression biomarkers; SD-OCT; late AMD

Citation: Flores R, Fradinho AC, Pereira RS, Mendes JM, Seabra MC, Tenreiro S, Carneiro Â. Identifying imaging predictors of intermediate age-related macular degeneration progression. Transl Vis Sci Technol. 2023;12(7):22, https://doi.org/10.1167/tvst.12.7.22

Purpose: Intermediate age-related macular degeneration (iAMD) is a risk factor for progression to advanced stages, but rates of progression vary between individuals. Predicting individual risk is advantageous for programing timely and effective treatment and for patient stratification into future clinical trials.

Methods: We conducted a prospective and noninterventional study following patients with iAMD for 24 months. Optical coherence tomography parameters related with drusen, hyper-reflective foci (HRF), presence of incomplete retinal pigment epithelial and outer retinal atrophy (iRORA) and ellipsoid zone (EZ) status were explored at the baseline. Patients were reclassified at the end of the follow-up period and divided according to their progression. A risk prediction model for progression to late AMD was developed.

Results: A total of 135 patients were enrolled in the study and 30.4% developed late disease. A multivariate logistic regression model was created using those optical coherence tomography parameters, further optimized by backward feature elimination. Parameters offering the best fit in prediction progression were presence of iRORA, EZ status, drusen area and presence of HRF. iRORA is the feature that provides a higher probability of developing late AMD (odds ratio, 12.91; $P = 0.000$), followed by EZ disruption status (odds ratio, 3.54; $P = 0.0018$). The area under the receiver operating characteristic curve calculated for the testing set was 0.77 (95% confidence interval, 0.56–0.98).

Conclusions: The combination of iRORA and EZ disruption constitute a high risk of progression to complete RORA within 2 years.

Translational Relevance: We propose a practical and useful model to help clinicians in their daily practice in predicting individual progression to advanced AMD.

Introduction

Age-related macular degeneration (AMD) is the leading cause of irreversible severe vision loss in individuals over 55 years old in the developed world.[1,2] Intermediate AMD (iAMD) is a risk factor for progression to advanced stages, but rates of progression vary between individuals. Interindividual progression rates of iAMD to advanced forms are extremely variable and currently there are no specific anatomical markers for disease progression that can predict individual risk of conversion to late AMD reliably.[3,4] If it was possible to preview progression to late AMD and to identify who might progress faster, this metric could be advantageous for programming timely and effective anti-vascular endothelial growth factor treatment for neovascular AMD (nAMD), for patient stratification into clinical trials for atrophic AMD, and, in the longer term, to allow better

personalized medicine if novel treatments emerge in the future.

Evaluation of drusen in color fundus photographs was, in the past, the main clinical standard for assessing patients with iAMD. There seems to be a positive correlation between the number, area, and extent of drusen observed in color fundus photographs and the risk of progression in more than 2 years.[5] Nevertheless, this method has limited value for predicting individual progression because it is unreliable in the short term.[5,6]

The recent widespread use of other noninvasive approaches in AMD retinal imaging has provided important tools in the identification of biomarkers of disease progression. With the aid of such multimodal retinal imaging modalities, clinicians and researchers are recognizing a wide range of image biomarkers of AMD progression.

Optical coherence tomography (OCT) indicates different types of drusen that may coexist in a patient, but their significance in AMD progression is still unknown.[7] Other OCT biomarkers related to progression to advanced AMD include drusen volume, hyper-reflective foci (HRF), reticular pseudo-drusen or subretinal drusenoid deposits, incomplete retinal pigment epithelial and outer retinal atrophy (iRORA), hypertransmission defects, and OCT-reflective drusen substructures.[8–10]

Several investigators using spectral domain OCT (SD-OCT) in patients with early and intermediate AMD reported that drusen area, height, and length predicted progression to advanced stages.[6] Baseline drusen volume is reported as an important factor of increased risk progression to either nAMD or geographic atrophy (GA).[11] Drusen height seems to have a positive correlation with progression to late atrophic AMD and drusen length with conversion to nAMD.[12] More recent SD-OCT volume studies provide more comprehensive measures.[13–18] Quantitative automatic determinations are available in some devices (Cirrus, Zeiss, Jena, Germany) whose role can be useful in clinical practice. Other devices have no automatic volume determinations (Spectralis, Heidelberg, Heidelberg, Germany) and drusen quantification volumes are dependent on OCT layer predictions and freely available nonapproved algorithms.[19,20]

HRF are discrete, well-defined lesions, with isoreflectvitiy or higher reflectivity than the retinal pigment epithelium (RPE). They are highly backscattering lesions located within the neurosensory retina, usually adjacent to the drusen edge or apex or in the inner neurosensory retina layers. They are described as representing extracellular pigment granules and outer segment debris (outer HRF) or displacement and clumping of degenerated RPE cells or microglia (inner HRF).[21] HRF are associated with increased risk for progression to advanced AMD,[8,22,23] and the presence of HRF is the strongest individual predictor for AMD progression.[22] In previous works, the number of HRF showed correlation with progression to late AMD,[22] in some studies with GA[10,11] and in others with macular neovascularization.[8,9]

Reticular pseudodrusen or subretinal drusenoid deposits are subretinal collections of granular, hyperreflective interlacing material located above the RPE. They are usually found in the superior macula or next to superotemporal arcades.[10] Near infrared reflectance (NIR) and SD-OCT seem to be particularly relevant and effective methods for diagnosing subretinal drusenoid deposits. Depending on the studied population, reticular pseudodrusen are present in approximately 9% to 58% of patients with iAMD.[24,25] The presence of reticular pseudodrusen is associated with an additional two- to six-fold increased risk of progression to advanced AMD, with the risk of progression being higher for reticular pseudodrusen located outside the macula.[24]

iRORA has replaced the so-called nascent GA in the new nomenclature obtained by the Consensus International Group (Classification of Atrophy Meeting).[26–30] Nascent GA corresponds with a localized loss of tissue in the outer retina layers without definite RPE loss and is defined, on OCT images, as a subsidence of the outer plexiform layer and the inner nuclear layer with a hyporeflective wedge.[31] iRORA, by definition, is related to the presence of hypertransmission (<250 µm), RPE attenuation or disruption, and photoreceptor degeneration. This finding was found in 22% of eyes with iAMD and in 7% of all AMD patients. iRORA is strongly associated with impending GA; an average of 11 months elapsed between early signs of nascent GA and the development of GA.[32] Hyper-transmission defects (the presence of increased transmission of signal below the RPE and into the choroid) and OCT-reflective drusen substructures (variation in the OCT drusen structure and properties) has also been proposed to be associated with an increased risk of AMD progression.[33] Their real prevalence in patients with iAMD and the associated risk of progression is still unknown. Finally, ellipsoid zone (EZ) disruption and focal RPE disruptions have also been associated with progression to advanced AMD and neovascularization.[34]

In this study, we followed a cohort of patients with iAMD for 24 months and we explore some markers of pathological retinal ageing that can predict individual progression to advanced stages. Particularly, we investigate and characterize drusen, HRF, and other

OCT features (presence of iRORA and EZ status) as biomarkers of disease progression and we calculate a risk prediction model for progression to late AMD, with estimates of sensitivity, specificity, and the receiver operating characteristic (ROC) curve analysis.

Methods

Study Design

This is a prospective, noninterventional study, with a follow-up of 24 months. Inclusion criteria at baseline were subjects older than 55 years with iAMD, selected from among the Retina Clinic of Ophthalmology department of "Centro Hospitalar Universitário de Lisboa Central," a tertiary hospital in Lisbon, Portugal. iAMD was defined based on Beckman classification[2,35,36] based on fundus lesions assessed within 2 disc diameters of the fovea. Eyes presenting large drusen (≥125 µm) or with pigmentary abnormalities associated with at least medium drusen (≥63 and <125 µm) were considered to have iAMD. Only one eye per patient was considered, even if both eyes were potentially eligible.

Patients were excluded if it was not possible to obtain a good image quality, if the refractive error was more than ±6 diopters or if there was any evidence of accumulation of extracellular fluid, hemorrhage, exudates, or fibrosis. Additional exclusion criteria included previous retinal surgery, laser treatment, history of glaucoma, signs of diabetic retinopathy, retinal vascular occlusion, hereditary retinal or macular dystrophy, and anti-vascular endothelial growth factor treatment in the study eye. In this prospective study, patients underwent a complete ophthalmologic evaluation, including best-corrected visual acuity, intraocular pressure, slit-lamp biomicroscopy, and 90D indirect fundoscopy. Color fundus photography, fundus autofluorescence, NIR, SD-OCT, and OCT angiography were performed in all patients and monitoring was perform every 6 months during the follow-up period.

A standardized imaging protocol was performed in all patients. For this cohort analysis, we included acquisition of combined (Figs. 1, 2, and 3):

(a) NIF images (λ = 815 nm, emission 700–1400 nm, field of view of 30° × 30°, and image resolution of 768 × 768 pixels);
(b) SD-OCT (λ = 870 nm, acquisition speed 40,000 A-scans per second, 20° × 20°, dense program, 512 × 49 scans, and spacing of 120 µm). The SD-OCT was acquired in combination with NIR allowing image overlapping.

Starting at the baseline at iAMD stage, patients were reclassified, at the end of the follow-up period, and divided according to their progression: stable or progression to late AMD (complete RORA [cRORA] or nAMD).

Ethics Issues

Participants who fulfilled the inclusion criteria were invited to participate and gave written informed

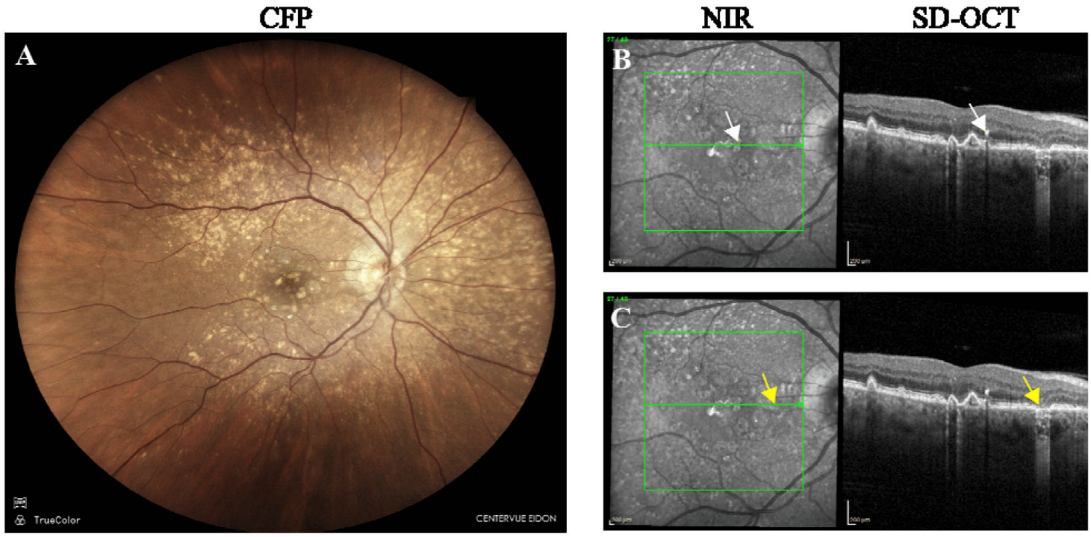

Figure 1. Representative images of (**A**) color fundus photographs, and the corresponding NIR and SD-OCT from an AMD patient in intermediate stage of the disease. (**B**) Example of HRF (*white arrows*) and (**C**) iRORA with hypertransmission, indicating RPE disruption and photoreceptor degeneration (*yellow arrows*).

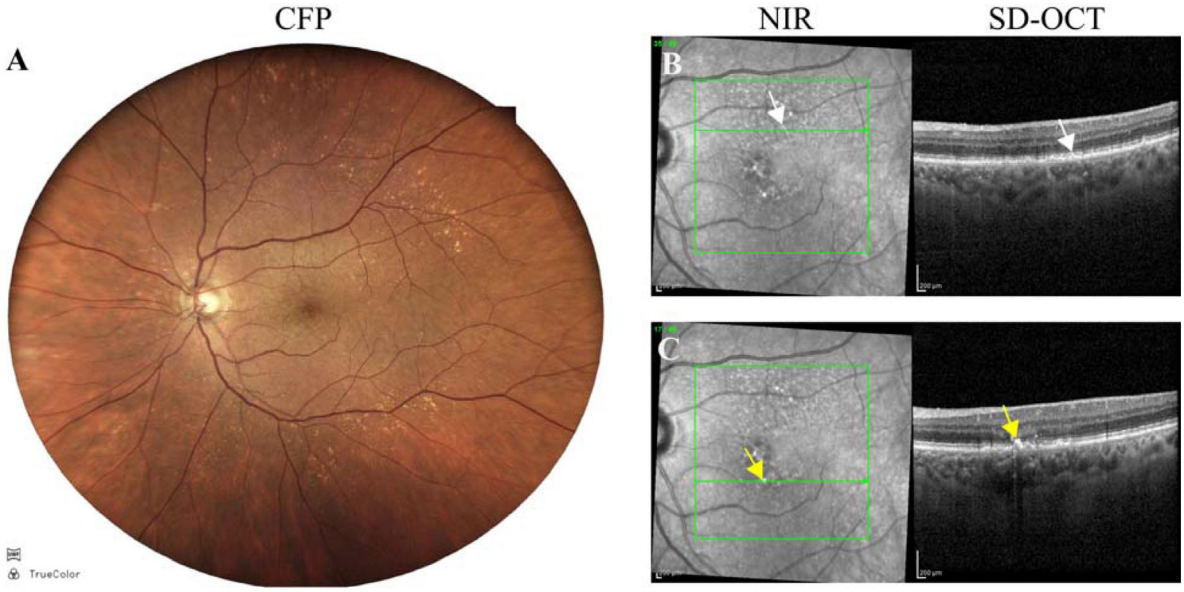

Figure 2. Representative images of (**A**) color fundus photographs, and the corresponding NIR and SD-OCT from an AMD patient in intermediate stage of the disease. (**B**) Example of subretinal drusenoid deposits (*white arrow*) and (**C**) hyperreflective drusen and adjacent HRF (*yellow arrows*).

consent after detailed explanation of the scope of the study. The protocol adhered to the tenets of the Declaration of Helsinki and was approved by the Ethic Commission of the "Centro Hospitalar Universitário de Lisboa Central."

Image Analysis and Measurements

For this investigational study, we manually analyzed OCT images (SD-OCT Spectralis, Heidelberg, Germany) at the baseline and at the end of the follow-up period. The SD-OCT was acquired in combination with NIR allowing image overlapping.

Drusen, HRF, and the other predefined OCT features in the outer retinal layers (presence of iRORA and EZ status) were analyzed. Subjective imagiologic features were evaluated and classified by two independent ophthalmologists. In the case of discrepancy, they discussed each dubious case and agreed on the final decision. The graders were masked as to the patient's clinical data not related with image analysis.

The drusen area was calculated using two perpendicular dimensions (length and height). Length was measured in the drusen base, and height was measured from the apex to the base in a perpendicular manner. Simultaneous scanning laser ophthalmoscopy images and overlaid enface NIR fundus images were used to ensure that the scan went through the center of an individual druse. Only those drusen that had been crossed in their center were included for the analysis. If the cross-section was off center, those drusen were not included in the analysis. We only considered for analysis the 10° × 10° area centered around the fovea and included in the analysis the drusen with the biggest area and the subfoveal one if present (approximately 500 µm).

Beside the drusen areas, we also studied drusen morphology, internal reflectivity, homogeneity, and the integrity of the EZ around the selected drusen. Assessment of incomplete RPE and outer retinal atrophy (iRORA) was considered. Concerning HRF, we analyzed their presence in the area 10° × 10° around the fovea, their number, location within the central 500 µm and association with drusen. Such metrics were also assessed at the follow-up OCT.

Statistical Analyses

Statistical analysis was performed in Python using the application Jupyter Notebooks version 6.4.5 from Anaconda. For each OCT feature, a comparison between groups (no disease progression/disease progression) was performed by nonparametric Mann–Whitney U test.

The association between all variables, including the target variable (0 [no progression] and 1 [progression to late AMD]), was assessed using Spearman's rank correlation coefficient (ρ). In this way, it was possible to assess if any of the SD-OCT features were correlated

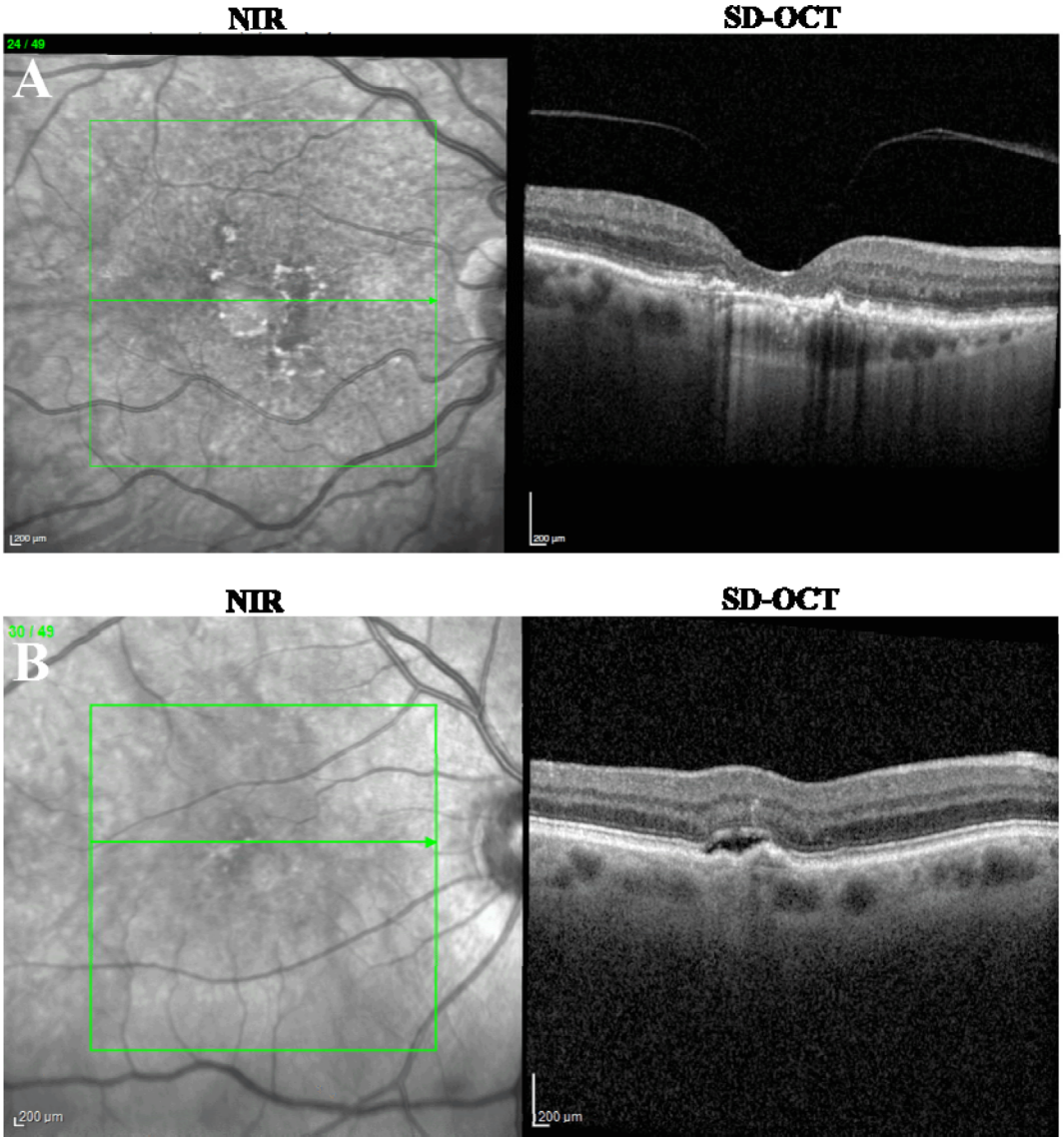

Figure 3. Representative images of NIR and SD-OCT from patients in advanced or late AMD. (**A**) An example of cRORA and (**B**) an example of nAMD.

among each other and with the outcome variable (i.e., disease progression). Among SD-OCT variables highly correlated ($\rho \geq 0.7$), only one of them was selected to be present in the multivariate logistic regression analysis. Additionally, it was applied k-fold cross-validation method (it was defined as $k = 5$) to resample our data and therefore evaluate the influence of each categorical variable within different subsets of our dataset. The importance of categorical variables within the dataset to the target variable was evaluated by the χ^2 test of independence, which tests whether two categorical variables are independent. Each independence test used a significance level of 5%.

Statsmodels is a Python module that provides *Logit*() function for performing logistic regression and statistical tests in the respective summary. A logit function models the probability of an event taking place by having its log-odds ratio as linear combination of one or more independent variables. Adjusted R2, Akaike's information criteria (AIC), and Bayesian information criterion (BIC) were used to evaluate the performance between logistic regressions. A multivariate logistic regression with the optimal subset of predictors was created using forward stepwise selection. Forward stepwise starts with a model that has no predictors and then adds predictors to it, one at a time. The variable that provides the greatest additional improvement to the fit was added to the model at each step. Statistical significance of coefficients was considered for a P value of less than 0.05.

To develop a logistic regression classifier to predict disease progression, a training and a testing set were

randomly selected (80% and 20% of the dataset, respectively). For the logistic regression classifier, a different approach was considered for selecting the best subset of variables. It used backward feature selection, whose main purpose is to examine the multivariate model and sequentially eliminate predictors that do not significantly impact the final outcome. Beginning with all potential predictors in the multivariate model, backward elimination sequentially keeps or discards variables according to a predetermined significance criterion (in our analysis F1-score was the evaluation measure for model selection). To quantify the performance of the logistic regression classifier with the selected variable predictors, the training dataset was divided using a stratified five-fold cross-validation, allowing to ensure that each of the five considered folds had the same proportion of observations. Additionally, several other evaluation metrics for the classification model were computed to assess model performance: (i) accuracy, (ii) balanced accuracy, (iii) precision, (iv) recall (or sensitivity), and (v) specificity.

Furthermore, the area under the curve of the ROC was calculated for the testing set never seen by the classifier. Note that this testing set has the same proportion of patients who progressed versus those who did not progress, as the entire dataset. The optimal cut-off point for late AMD predictions was estimated as the value that warranted the highest of true positive rate (sensitivity), while maintaining a low false positive rate (1 – specificity).

Results

A total of 135 eyes of 135 patients with iAMD were considered in this study. Patient (55 men and 80 women) ages ranged from 57 to 98 years. Image

Table 1. SD-OCT Features at Baseline for the Groups of Patients Where No Progression was Observed vs. Where Evolution to Late AMD was Found

SD-OCT Features	No Progression	Progression to Late AMD	*P* Value
iRORA	No – 91.5% Yes – 8.5%	No – 61.0% Yes – 39.0%	**1×10^{-10}**
Drusen morphology	Serous –59.6% Reticular or both - 40.4%	Serous – 58.5% Reticular or both - 41.5%	0.913
Central drusen (within 0.5 mm)	Yes – 42.6% No – 57.4%	Yes – 46.3% No – 53.7%	0.686
Subfoveal drusen area (μm^2)	39559.5 (21027.3 – 100811.5)	26002 (17314 – 53435)	0.166
Other drusen area (μm^2)	35967.5 (23946–57165.8)	35853 (27894.3–57000.8)	0.516
Drusen reflectivity	Low – 6.4% Intermediate – 69.1% High – 24.5%	Low – 7.3% Intermediate – 75.6% High – 17.1%	0.377
Drusen homogeneity	Homogeneous – 84.0% Heterogeneous – 16.0%	Homogeneous – 75.6% Heterogeneous – 24.4%	0.249
EZ disruption	No – 86.2% Yes – 13.8%	No – 58.5% Yes – 41.5%	**0.0004**
HRF	No – 59.6% Yes – 40.4%	No – 19.5% Yes – 80.5%	**0.00002**
No. of HRF	0 – 60.6% 1 – 6.4% 2-5 – 22.3% $\geq$ 6 – 10.6%	0 – 19.5% 1 – 12.2% 2-5 – 34.1% $\geq$ 6 – 34.1%	**0.000007**
HRF location (within 500-µm disc area)	No – 86.2% Yes – 13.8%	No – 82.9% Yes – 17.1%	0.630
HRF association to drusen	No – 63.8% Yes – 36.2%	No – 34.1% Yes – 65.9%	**0.002**

Mann–Whitney *U* test. The level of significance was set at $P < 0.05$. Significant values are in bold.

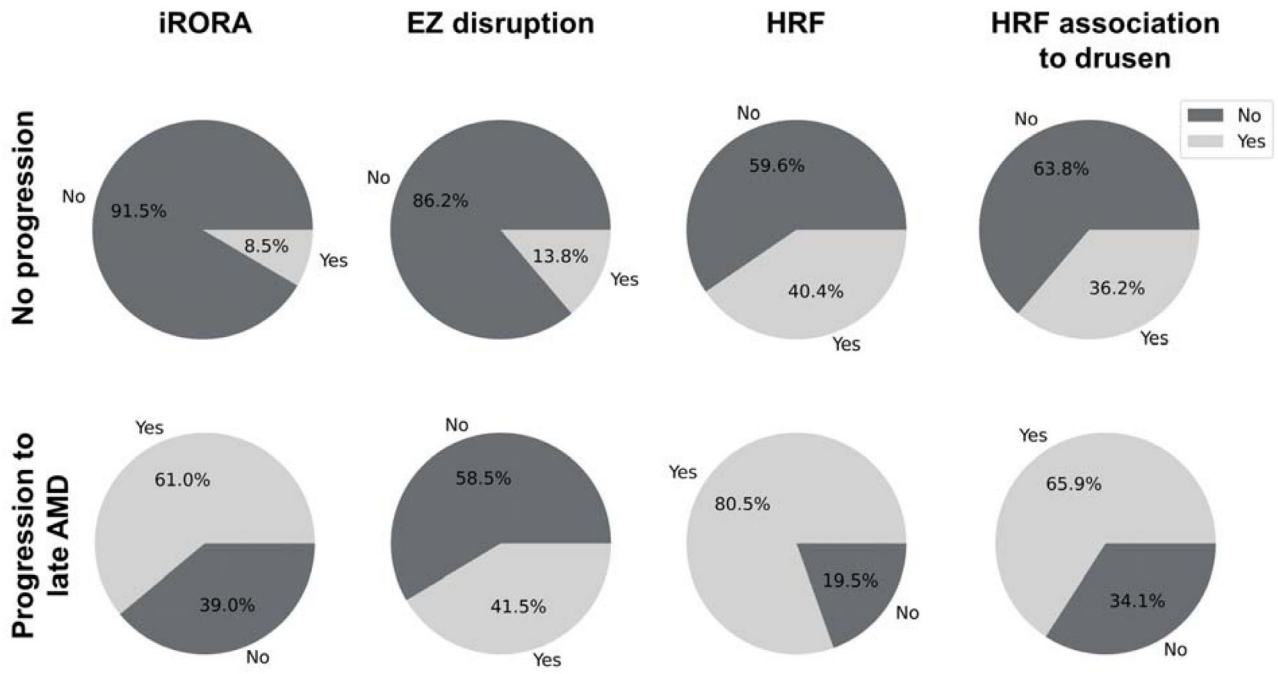

Figure 4. Pie charts of binary SD-OCT variables which revealed a statistically significant difference between the groups of patients that progressed to late AMD versus those that remained in intermediate AMD.

analysis was performed by two experts and interobserver agreement was substantially favorable (>90%) for SD-OCT measured parameters related with drusen and with HRF; classification of progression was also congruent among both ophthalmologists.

Considering disease progression, 30.4% of the patients ($n = 41$) developed cRORA or nAMD and the remaining 69.6% ($n = 94$) did not progress to late AMD forms. We analyzed 238 drusen and classified them considering size, morphology, internal reflectivity, homogeneity, and integrity of the EZ around the selected drusen. At baseline, drusen areas ranged from 23,481.25 μm^2 to 62,010.25 μm^2 (median [Q1–Q3]). Of the patients, 31.9% presented subfoveal drusen (located within central 500 µm) at baseline. Regarding HRF, they were found in 52.6% at baseline of our cohort and most of those patients presented two to five HRF in the predefined area. These imaging features were assessed at baseline in the two groups of patients (no progression vs. progression to late AMD). The overall assessment is shown in Table 1.

At baseline, the Mann–Whitney U test revealed statistically significant differences in the following features: iRORA, EZ disruption, number of HRF, HRF, and HRF association with drusen, between the group of patients that developed late AMD and the group that did not progress to advanced forms of AMD (Figs. 4 and 5).

Filter methods (Spearman correlation and χ^2 test of independence) provided an initial approach to

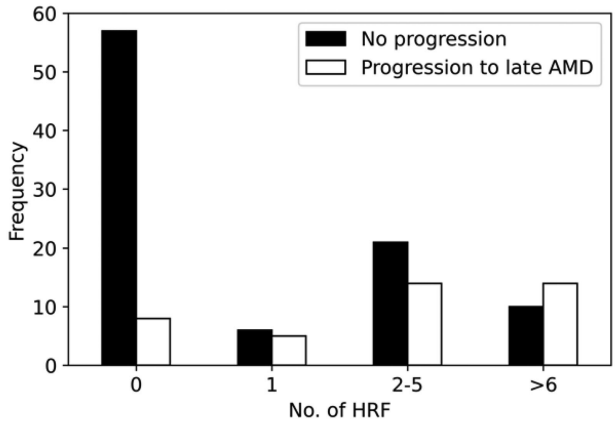

Figure 5. Bar plot shows the number of HRF found at the baseline in groups where disease progression was observed (*white*) and where AMD remained in the intermediate phase (*black*).

the data to assess the correlation among SD-OCT variables. HRF, number of HRF, and HRF association with drusen were very strongly correlated among each other ($\rho \geq 0.8$). The χ^2 test showed that categorical variables, iRORA, EZ disruption, HRF, number of HRF, and HRF association with drusen were important for the prediction model. Additionally, univariate logistic regressions were performed for each SD-OCT feature to determine which candidate predictors correlate significantly with the outcome. The SD-OCT features whose coefficients showed statistical significance were iRORA, EZ disruption, HRF,

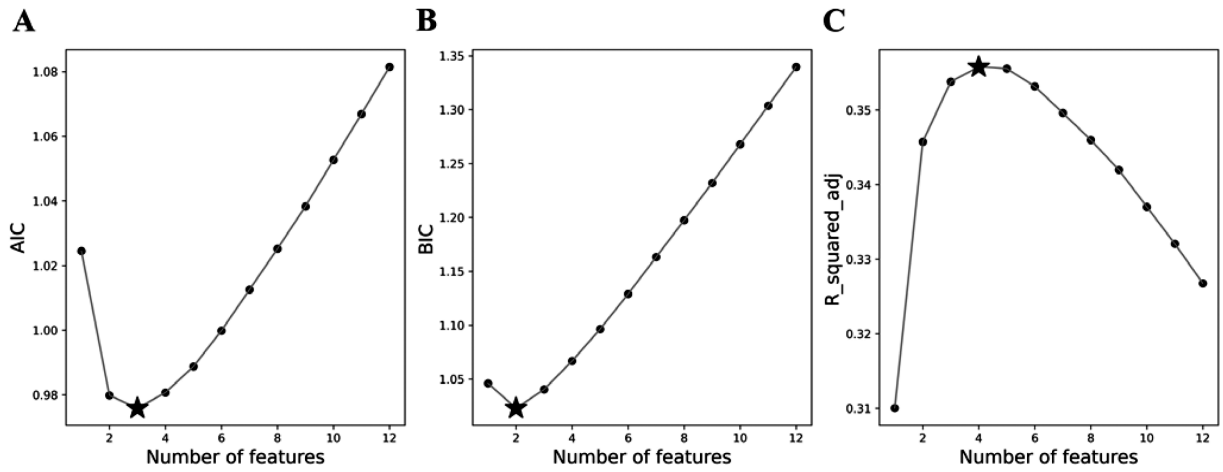

Figure 6. The logistic regression models created by forward stepwise selection were evaluated with (**A**) AIC, (**B**) BIC and (**C**) adjusted R^2. The best model according to each criterion is marked with a star.

Table 2. Results of Logistic Regression Analysis

SD-OCT Variables	b_r (Estimator Coefficients)	*P* Value	Odds Ratio
iRORA	2.5576	**0.00002**	12.905
EZ disruption	1.2627	**0.018**	3.535
Drusen area	1.5137	0.216	4.544
HRF	0.6295	0.243	1.878

Significant values are in bold.

number of HRF, and HRF association with drusen ($p < 0.05$) in agreement with Table 1.

The 12 models created by forward stepwise selection can be seen in Supplementary Table 1. The best models were composed by three (iRORA, EZ disruption, drusen area) using AIC criteria (Fig. 6A) or 2 (iRORA, EZ disruption) predictor variables using BIC criteria (Fig. 6B), respectively. However, the model with four predictor variables (iRORA, EZ disruption, drusen area, and HRF) evidenced the highest adjusted R2 (0.3558) (Fig. 6C), that is, this set of predictors was the best one to explain the variation in the outcome variable (disease progression), without considerably increasing AIC and BIC, as observed in Figure 6.

A multivariate logistic regression with the aforementioned SD-OCT variables was created to ascertain the effects of each variable (while holding the remaining variables at a fixed value) on the likelihood that patients would remain in iAMD or progress to late AMD forms (Table 2). The fitted model indicated that the odds of developing late AMD for patients who have iRORA over the odds of patients that do not exhibit atrophy is 12.91 ($P = 0.000$). The odds for patients with iRORA constitute approximately a 12-fold increase in comparison with the odds for patients who do not have it. Similarly, the odds of evolving to advanced AMD is 3.54 for patients whose EZ is disrupted versus those whose EZ integrity is maintained, indicating a 2.5-fold increase in developing late AMD for patients who have a disruption in the EZ ($P = 0.018$).

Concerning the development of a logistic regression classifier, through backward feature selection, the subset with the highest F1-score was composed of six variables, namely, drusen morphology, iRORA, drusen area, EZ disruption, HRF, and HRF in central location (Supplementary Fig. 1). The F1-score of the designated model with the five-fold cross-validation was 0.707 ± 0.02 in the training set and 0.731 ± 0.08 in the validation set. On the testing set, the F1-score was 0.67.

The evaluation metrics averages for the training and validation datasets and the exact values for the testing subset is presented in the supplementary Table 2. The area under the ROC curve calculated for the testing set was 0.77 (95% confidence interval, 0.56–0.98) (Fig. 7). The optimal cut-off value was 0.68 (sensitivity, 0.75; specificity, 0.79); that is, if the predicted probability of developing late AMD is greater than 0.68, that observation is classified as 1, or a patient whose iAMD will progress to late AMD.

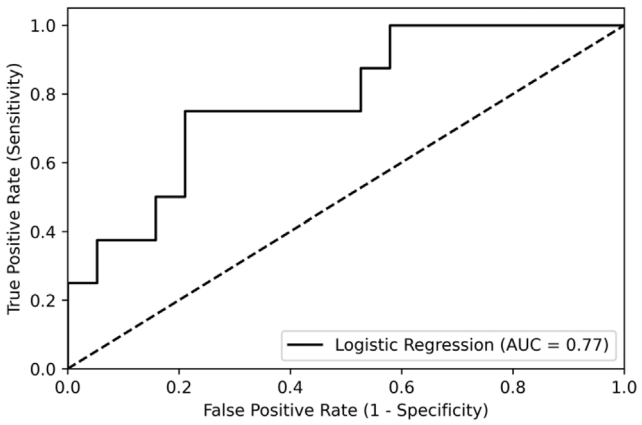

Figure 7. ROC curve for disease prediction model performance using "Drusen morphology," "iRORA," "Drusen area," "EZ disruption," "HRF" and "HRF in central location" parameters. ROC curve (*solid line*) was plotted using the testing dataset and the area under the curve was calculated: area under the curve = 0.77). The *dashed diagonal line* serves as an imaginary reference line representing a nondiscriminatory test.

Discussion

Here we present a practical and useful clinical model to help clinicians in their daily practice in predicting individual progression to advanced AMD. The main conclusion of our study is that some key imaging parameters are able to predict AMD progression.

In this study, 30.4% of our patients progressed to advanced disease, a percentage higher than expected considering similar studies.[37] One possible reason for this finding is the patients' mean age of our cohort: 80.23 years old (median, 81 ± 8.17 years of age). It is a particularly elderly population with a known increased risk of progression. Another important consideration is that the percentage of patients with advanced disease in the fellow eye in our study at baseline was 25.9%. Previous studies have also documented that the presence of advanced AMD in the fellow eye at baseline increased the rates of progression to advanced AMD in study eyes.[38] Finally, all our intermediate AMD patients are under Age-Related Eye Disease Study vitamin supplementation, but we noticed that it was not the rule before referring to our center.

In this study, the presence of iRORA and the disruption of the EZ were SD-OCT features that emerged as having a significant association in predicting disease progression over a period of 2 years, even in the multivariate analysis. The individual predictor, iRORA, was found to account for approximately 31% of the variability observed in the dependent variable (disease progression). This finding suggested that iRORA was the most influential predictor variable. The addition of three more variables, specifically the EZ disruption variable, contributed to a 5% increase in the overall explanatory power of the model, which led to more accurate predictions. The addition of more variables should be considered when they are not highly correlated with the already existing variables in the model, to avoid the risk of multicollinearity and the consequent misleading interpretation of beta estimators. However, if they increase the explanatory power of the model, their addition should be considered. Still, it was important to assess the trade-off between model complexity (i.e., many variables) and predictive power of the model when selecting whether to incorporate more variables or not. Having this balance in mind, the model that reflected the best trade-off was the one shown for the multivariate analysis. In this model, the odds of patients presenting with iRORA developing late AMD were 12-fold higher than the odds for those who did not. Additionally, the odds for patients with EZ disrupted were 254% higher than the odds for those whose EZ integrity was maintained (2.5-fold higher).

These results are understandable if we report to features required to define iRORA definition, which include choroidal hypertransmission, disruption of the RPE, and degeneration of photoreceptors. One of the signs of photoreceptors degeneration is, really, EZ disruption, but others can be considered in iRORA definition as external limiting membrane disruption, outer nuclear layer disruption, and subsidence of the outer plexiform layer and the inner nuclear layer with a hyporeflective wedge.

Furthermore, the presence of HRF and their number or association to drusen, showed statistically significant correlation with disease progression. Owing to multicollinearity issues, only the presence of HRF was selected to be present in the multivariate logistic regression. Interestingly, when iRORA, EZ disruption, and drusen area were held constant, the presence of HRF no longer predicted the outcome significantly. One may hypothesize that the presence of HRF were only predictive because of its associations with other predictors or because the other parameters are more significantly related with disease progression.

The area under the ROC curve calculated for the testing set in our study was 0.77 (95% confidence interval, 0.56–0.98), which is considered good discrimination for predicting disease progression. The inclusion and analysis of other imaging parameters, such as vascular parameters obtained by OCT angiography, in a multimodal approach could possibly increase the performance of the model.

We also analyzed whether the study could predict progression toward subtypes of advanced AMD

(cRORA or nAMD). The multiclass logistic regression model correctly identified four of five patients whose disease had progressed to cRORA but failed to correctly identify (0/3) nAMD patients in a randomly selected testing set. One may speculate that the SD-OCT variables collected in this study are more related with atrophic features, and, hence the correct prediction of cRORA development, compared with the relative weakness in predicting strictly neovascular progression. Therefore, the addition of vascular parameters evaluated by OCT angiography (nonexudative macular neovascularization) may not only increase the robustness of the prediction model, but also predict development of nAMD correctly.

A recent study provided support to the hypothesis that iRORA could be considered a common risk factor in eyes with intermediate AMD patients for development of atrophic late disease.[39] We still need more data to understand its definite value, as a risk factor for predicting AMD progression from intermediate to advanced atrophic stage, particularly when considered alongside other well-known fundoscopic risk factors, such as large drusen and pigmentary abnormalities.

The MACUSTAR clinical study is a low interventional clinical multicentric study that was designed to develop and evaluate functional, structural, and patient-reported outcome measures, that will improve our understanding of natural history and prognostic markers of iAMD progression, with aims to be used in future clinical trials. It included a longitudinal and cross-sectional arm, beginning in September 2017, with the end date programed in February 2024.[40–42] One other important study, the PINNACLE, has been designed as a large-scale, retrospective, and prospective study, noninterventional and multicenter, and is still running in multiple sites in United Kingdom, Austria, and Switzerland.[43] Its main goal is the identification of prediction biomarkers and to report the natural history of progression of iAMD with multimodal retinal imaging. This study also combines both machine learning and retrospective and prospective AMD patient data.[43]

Our study shares similarities with MACUSTAR and PINNACLE concerning primary and secondary outcomes, although it is mainly prospective, with a smaller sample and shorter follow-up, and image analyses were not obtained by automatic procedures such as deep or machine learning models. It also does not include functional or patient-reported outcomes data. It will be interesting, in the near future, to compare our results with larger and longer studies, as those obtained by MACUSTAR and PINNACLE.[40–43]

This study has some considerable limitations; those related with the follow-up period and sample size are important issues, particularly in such a chronic and prevalent disease as AMD. Another important weakness was the inclusion of SD-OCT images, excluding the potential value of swept source OCT technology. The exclusive manual analysis used in this study is also an important limitation and automatic image analysis methods, as those obtained by artificial intelligence methods, should add interesting data and a tool to be considered in the near future.

Future work includes the need to extend the sample and the follow-up period, as well as considering the analysis of more image parameters in a multimodal approach for this cohort. Additionally, the human observation used here may soon be substituted by artificial intelligence methods. Deep learning models generally achieve high performances, comparable with that of individual specialists.[44,45] Those models reveal significant potential to improve the quality and accessibility of ophthalmic care, but they use parameters that are sometimes difficult to apply in clinical practice and need further external validation to be performed in the near future.[46]

In summary, we believe the results of this study are robust enough to allow us to propose a practical and useful clinical model to guide clinicians in daily practice, using simple tomographic parameters. The present study suggests that the combination of iRORA and EZ disruption constitute a high risk of progression to cRORA within two years. We aim to continue to develop a scoring system that may facilitate general ophthalmologists in the identification of patients with iAMD with a high risk of progressing to advanced stage of disease. Quantifying markers of pathological retinal ageing predictive of individual progression to advanced AMD is an appealing goal toward personalized risk assessment in AMD.

Acknowledgments

Supported by iNOVA4Health – UIDB/04462/2020 and UIDP/04462/2020, and by the Associated Laboratory LS4FUTURE (LA/P/0087/2020), two programs financially supported by Fundação para a Ciência e Tecnologia (FCT)/Ministério da Ciência, Tecnologia e Ensino Superior. ACF was recipient of individual PhD fellowship funded by FCT (PD/BD/135503/2018).

Disclosure: **R. Flores**, None; **A.C. Fradinho**, None; **R.S. Pereira**, None; **J.M. Mendes**, None; **M.C. Seabra**, None; **S. Tenreiro**, None; **Â. Carneiro**, None

References

1. Li JQ, Welchowski T, Schmid M, Mauschitz MM, Holz FG, Finger RP. Prevalence and incidence of age-related macular degeneration in Europe: a systematic review and meta-analysis. *Br J Ophthalmol*. 2020;104(8):1077–1084.
2. Ferris FL, Wilkinson CP, Bird A, et al. Clinical classification of age-related macular degeneration. *Ophthalmology*. 2013;120(4):844–851.
3. Sunness JS, Margalit E, Srikumaran D, et al. The long-term natural history of geographic atrophy from age-related macular degeneration. Enlargement of atrophy and implications for interventional clinical trials. *Ophthalmology*. 2007;114(2):271–277.
4. Schmitz-Valckenberg S, Sahel JA, Danis R, et al. Natural history of geographic atrophy progression secondary to age-related macular degeneration (Geographic Atrophy Progression Study). *Ophthalmology*. 2016;123(2):361–368.
5. Friberg TR, Bilonick RA, Brennen PM. Analysis of the relationship between drusen size and drusen area in eyes with age-related macular degeneration. *Ophthalmic Surg Lasers Imaging*. 2011;42(5):369–375.
6. de Sisternes L, Simon N, Tibshirani R, Leng T, Rubin DL. Quantitative SD-OCT imaging biomarkers as indicators of age-related macular degeneration progression. *Invest Ophthalmol Vis Sci*. 2014;55(11):7093–7103.
7. Khanifar AA, Koreishi AF, Izatt JA, Toth CA. Drusen ultrastructure imaging with spectral domain optical coherence tomography in age-related macular degeneration. *Ophthalmology*. 2008;115(11):1883–1890.
8. Nassisi M, Lei J, Abdelfattah NS, et al. OCT risk factors for development of late age-related macular degeneration in the fellow eyes of patients enrolled in the HARBOR study. *Ophthalmology*. 2019;126(12):1667–1674.
9. Christenbury JG, Folgar FA, O'Connell R V., Chiu SJ, Farsiu S, Toth CA. Progression of intermediate age-related macular degeneration with proliferation and inner retinal migration of hyperreflective foci. *Ophthalmology*. 2013;120(5):1038–1045.
10. Flores R, Carneiro Â, Tenreiro S, Seabra MC. Retinal progression biomarkers of early and intermediate age-related macular degeneration. *Life*. 2022;12(1):36.
11. Nathoo NA, Or C, Young M, et al. Optical coherence tomography-based measurement of drusen load predicts development of advanced age-related macular degeneration. *Am J Ophthalmol*. 2014;158(4):757–761.e1.
12. Dieaconescu DA, Dieaconescu IM, Williams MA, Hogg RE, Chakravarthy U. Drusen height and width are highly predictive markers for progression to neovascular AMD. *Invest Ophthalmol Vis Sci*. 2012;53(14):2910–2910.
13. Yehoshua Z, Wang F, Rosenfeld PJ, Penha FM, Feuer WJ, Gregori G. Natural history of drusen morphology in age-related macular degeneration using spectral domain optical coherence tomography. *Ophthalmology*. 2011;118(12):2434–2441.
14. Corvi F, Srinivas S, Nittala MG, et al. Reproducibility of qualitative assessment of drusen volume in eyes with age related macular degeneration. *Eye*. 2021;35(9):2594–2600.
15. Schlanitz FG, Baumann B, Kundi M, et al. Drusen volume development over time and its relevance to the course of age-related macular degeneration. *Br J Ophthalmol*. 2017;101(2):198–203.
16. Diniz B, Rodger DC, Chavali VR, et al. Drusen and RPE atrophy automated quantification by optical coherence tomography in an elderly population. *Eye*. 2015;29(2):272–279.
17. De Amorim Garcia Filho CA, Yehoshua Z, Gregori G, et al. Change in drusen volume as a novel clinical trial endpoint for the study of complement inhibition in age-related macular degeneration. *Ophthalmic Surg Lasers Imaging Retina*. 2014;45:18–31.
18. Murthy Chavali VR, Diniz B, Diniz B, et al. Association of oct-derived drusen measurements with AMD-associated genotypic SNPs in the Amish population. *J Clin Med*. 2015;4(2):304–317.
19. Garzone D, Terheyden JH, Morelle O, et al. Comparability of automated drusen volume measurements in age-related macular degeneration: a MACUSTAR study report. *Sci Rep*. 2022;12(1):1–10.
20. Wintergerst MWM, Gorgi Zadeh S, Wiens V, et al. Replication and refinement of an algorithm for automated drusen segmentation on optical coherence tomography. *Sci Rep*. 2020;10(1):1–7.
21. Curcio CA, Zanzottera EC, Ach T, Balaratnasingam C, Freund KB. Activated retinal pigment epithelium, an optical coherence tomography biomarker for progression in age-related macular degeneration. *Invest Ophthalmol Vis Sci*. 2017;58(6):BIO211–BIO226.
22. Nassisi M, Fan W, Shi Y, et al. Quantity of intraretinal hyperreflective foci in patients with intermediate age-related macular degeneration correlates with 1-year progression. *Invest Ophthalmol Vis Sci*. 2018;59(8):3431–3439.

23. Lei J, Balasubramanian S, Abdelfattah NS, Nittala MG, Sadda SR. Proposal of a simple optical coherence tomography-based scoring system for progression of age-related macular degeneration. *Graefes Arch Clin Exp Ophthalmol*. 2017;255(8):1551–1558.
24. Zweifel SA, Imamura Y, Spaide TC, Fujiwara T, Spaide RF. Prevalence and significance of subretinal drusenoid deposits (reticular pseudodrusen) in age-related macular degeneration. *Ophthalmology*. 2010;117(9):1775–1781.
25. Ly A, Yapp M, Nivison-Smith L, Assaad N, Hennessy M, Kalloniatis M. Developing prognostic biomarkers in intermediate age-related macular degeneration: their clinical use in predicting progression. *Clin Exp Optom*. 2018;101(2):172–181.
26. Holz FG, Sadda SVR, Staurenghi G, et al. Imaging protocols in clinical studies in advanced age-related macular degeneration: recommendations from Classification of Atrophy Consensus Meetings. *Ophthalmology*. 2017;124:464–478.
27. Sadda SR, Guymer R, Holz FG, et al. Consensus definition for atrophy associated with age-related macular degeneration on OCT: Classification of Atrophy Report 3. *Ophthalmology*. 2018;125(4):537–548.
28. Guymer RH, Rosenfeld PJ, Curcio CA, et al. Incomplete retinal pigment epithelial and outer retinal atrophy in age-related macular degeneration: Classification of Atrophy Meeting Report 4. *Ophthalmology*. 2020;127:394–409.
29. Jaffe GJ, Chakravarthy U, Freund KB, et al. Imaging features associated with progression to geographic atrophy in age-related macular degeneration: Classification of Atrophy Meeting Report 5. *Ophthalmol Retina*. 2021;5:855–867.
30. Wu Z, Pfau M, Blodi BA, et al. OCT signs of early atrophy in age-related macular degeneration: interreader agreement: Classification of Atrophy Meetings Report 6. *Ophthalmol Retina*. 2022;6:4–14.
31. Monés J, Biarnés M, Trindade F. Hyporeflective wedge-shaped band in geographic atrophy secondary to age-related macular degeneration: an underreported finding. *Ophthalmology*. 2012;119(7):1412–1419.
32. Wu Z, Luu CD, Ayton LN, et al. Optical coherence tomography-defined changes preceding the development of drusen-associated atrophy in age-related macular degeneration. *Ophthalmology*. 2014;121(12):2415–2422.
33. Veerappan M, El-Hage-Sleiman AKM, Tai V, et al. Optical coherence tomography reflective drusen substructures predict progression to geographic atrophy in age-related macular degeneration. *Ophthalmology*. 2016;123(12):2554–2570.
34. Ferrara D, Silver RE, Louzada RN, Novais EA, Collins GK, Seddon JM. Optical coherence tomography features preceding the onset of advanced age-related macular degeneration. *Invest Ophthalmol Vis Sci*. 2017;58(9):3519–3529.
35. Bressler SB, Bressler NM. *Age-Related Macular Degeneration: Non-Neovascular Early AMD, Intermediate AMD, and Geographic Atrophy*. 5th ed. In: Ryan SJ, Hinton DR, Sadda SR, Wiedemann P, Schachat AP, Wilkinson CP, eds. New York: Elsevier Inc.; 2013.
36. Thee EF, Meester-Smoor MA, Luttikhuizen DT, et al. Performance of classification systems for age-related macular degeneration in the Rotterdam study. *Transl Vis Sci Technol*. 2020;9(2):1–11.
37. Vitale S, Agrón E, Clemons TE, et al. Association of 2-year progression along the AREDS AMD scale and development of late age-related macular degeneration or loss of visual acuity: AREDS report 41. *JAMA Ophthalmol*. 2020;138(6):610–617.
38. Chew EY, Clemons TE, Agrón E, et al. Ten-year follow-up of age-related macular degeneration in the Age-Related Eye Disease Study: AREDS report no. 36. *JAMA Ophthalmol*. 2014;132(3):272–277.
39. Wu Z, Goh KL, Hodgson LAB, Guymer RH. Incomplete retinal pigment epithelial and outer retinal atrophy: longitudinal evaluation in age-related macular degeneration. *Ophthalmology*. 2023;130(2):205–212.
40. Terheyden JH, Holz FG, Schmitz-Valckenberg S, et al. Clinical study protocol for a low-interventional study in intermediate age-related macular degeneration developing novel clinical endpoints for interventional clinical trials with a regulatory and patient access intention - MACUSTAR. *Trials*. 2020;21(1):659.
41. Finger RP, Schmitz-Valckenberg S, Schmid M, et al. MACUSTAR: development and clinical validation of functional, structural, and patient-reported endpoints in intermediate age-related macular degeneration. *Ophthalmologica*. 2019;241(2):61–72.
42. Saßmannshausen M, Behning C, Weinz J, et al. Characteristics and spatial distribution of structural features in age-related macular degeneration: a MACUSTAR Study report. *Ophthalmol Retina*. 2023;7(5):420–430. Published online December 2023.
43. Sutton J, Menten MJ, Riedl S, et al. Developing and validating a multivariable prediction model

which predicts progression of intermediate to late age-related macular degeneration—the PINNACLE trial protocol. *Eye*. 2023;37(6):1275–1283. Published online 2022.

44. Liu X, Faes L, Kale AU, et al. A comparison of deep learning performance against health-care professionals in detecting diseases from medical imaging: a systematic review and meta-analysis. *Lancet Digit Heal*. 2019;1(6):e271–e297.
45. Damian I, Nicoară SD. SD-OCT biomarkers and the current status of artificial intelligence in predicting progression from intermediate to advanced AMD. *Life*. 2022;12(3):454.
46. Paul SK, Pan I, Sobol WM. A systematic review of deep learning applications for optical coherence tomography in age-related macular degeneration. *Retina*. 2022;42(8):1417–1424.